Hohmann Spiral Transfer With Inclination Change Performed By Low-Thrust System

Steven Owens[1] and Malcolm Macdonald[2]

This paper investigates the Hohmann Spiral Transfer (HST), an orbit transfer method previously developed by the authors incorporating both high and low-thrust propulsion systems, using the low-thrust system to perform an inclination change as well as orbit transfer. The HST is similar to the bi-elliptic transfer as the high-thrust system is first used to propel the spacecraft beyond the target where it is used again to circularize at an intermediate orbit. The low-thrust system is then activated and, while maintaining this orbit altitude, used to change the orbit inclination to suit the mission specification. The low-thrust system is then used again to reduce the spacecraft altitude by spiraling in-toward the target orbit. An analytical analysis of the HST utilizing the low-thrust system for the inclination change is performed which allows a critical specific impulse ratio to be derived determining the point at which the HST consumes the same amount of fuel as the Hohmann transfer. A critical ratio is found for both a circular and elliptical initial orbit. These equations are validated by a numerical approach before being compared to the HST utilizing the high-thrust system to perform the inclination change. An additional critical ratio comparing the HST utilizing the low-thrust system for the inclination change with its high-thrust counterpart is derived and by using these three critical ratios together, it can be determined when each transfer offers the lowest fuel mass consumption. Initial analyses have shown the HST utilizing low-thrust inclination change to offer the greatest benefit at low $R2$ ($R2 \rightarrow R1$) and large ΔI ($\Delta I > 30°$). A novel numerical optimization process which could be used to optimize the trajectory is also introduced.

INTRODUCTION

As commercial satellites have an ever-increasing role in our everyday lives there is great demand for more satellite platforms to accommodate the services offered such as telecommunications, Global Positioning System (GPS) and Earth-monitoring. As the life length of such a platform is largely dictated by its amount of on-board fuel there is great interest in ensuring the fuel required for the trajectory to deliver the satellite to its working orbit is kept at a minimum. This paper investigates the Hohmann Spiral Transfer (HST), an orbit transfer method previously developed by the author incorporating both high and low-thrust propulsion systems[1–3], with an inclination change performed by the low-thrust propulsion system. The HST is similar to a bi-elliptic transfer as the high-thrust system is first used to propel the spacecraft way beyond the target where it is used again to circularize at an intermediate orbit. The low-thrust system is then activated and, while maintaining this orbit altitude, used to change the orbit inclination to suit the mission specification. The low-thrust system is then used again to reduce the spacecraft altitude and spiral

---

[1] Mr, Advanced Space Concepts Laboratory, Mechanical and Aerospace Department, University of Strathclyde, PhD Research Student, Lord Hope Building, 141 St James Road, Glasgow, G4 0LT

[2] Dr, Advanced Space Concepts Laboratory, Mechanical and Aerospace Department, University of Strathclyde, Senior Lecturer, Lord Hope Building, 141 St James Road, Glasgow, G4 0LT

in toward the target orbit. Figure 1 gives a visual representation of the transfer. The analytical methodology is compared to a numerical method for validation before being compared against the HST using the high-thrust system to impart the inclination change, as described in Reference 1, to determine when each transfer should be used.
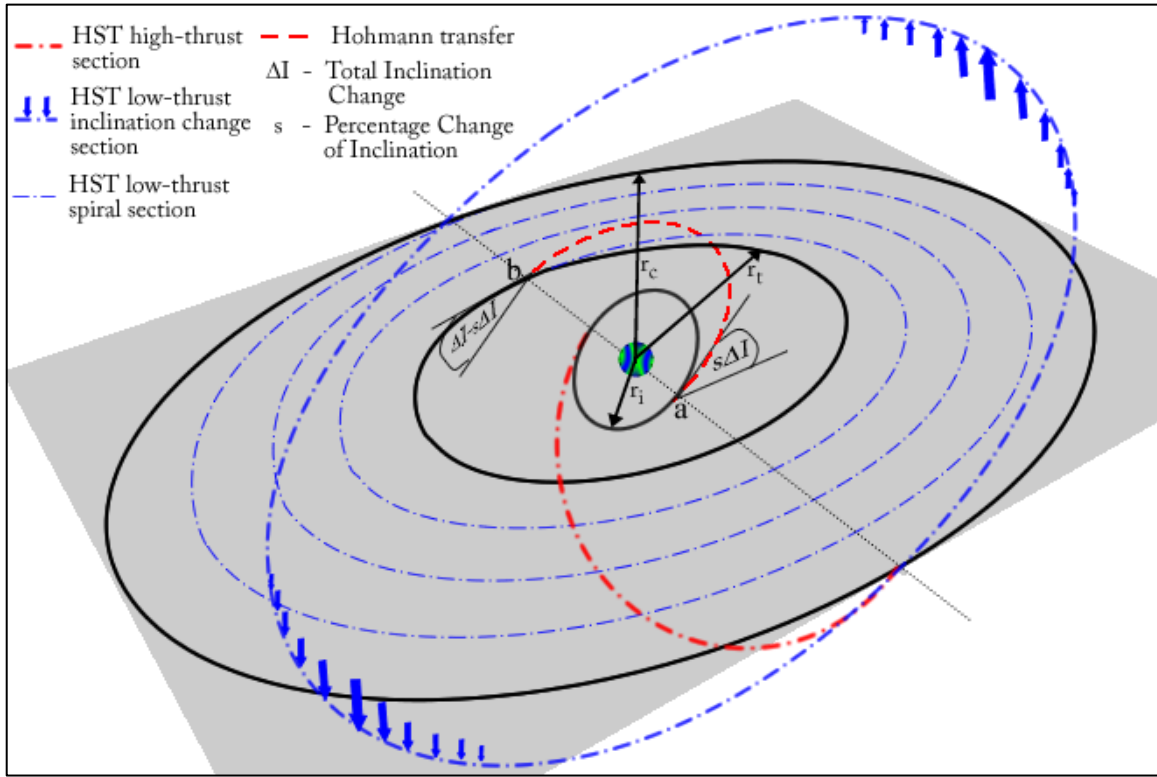

Figure 1. HST and Hohmann Transfer Specification

CRITICAL SPECIFIC IMPULSE DERIVATION

The critical ratios for the HST and compared transfers are referred to as I_{sp}^{XXXX}, where the superscript section denotes the comparison as is detailed in Table 3. They are considered separately as different orbit transfers will depend on one ratio and not the other. The analytical equations derived in this paper only concern the HST with low-thrust inclination change.

The following equations derive the critical specific impulse ratio, which can then be applied to each case independently. The high thrust and HST fuel mass fractions can be written as,

$$\frac{m_{HF}}{m_{wet}} = 1 - exp^{\left(\frac{-\Delta V_{H(C/E)}}{gI_{spH}}\right)} \tag{1}$$

$$\frac{m_{HSTF}}{m_{wet}} = 1 - exp^{\left(\frac{-\Delta V_{HSTH(C/E)}}{gI_{spH}}\right)} exp^{\left(\frac{-\Delta V_{HSTL}}{gI_{spL}}\right)} \tag{2}$$

By equating Eqns. (1) and (2), it can be shown that the HST transfer is equivalent, or better in terms of fuel mass fraction when,

$$exp^{\left(\frac{-\Delta V_{H(C/E)}}{gI_{spH}}\right)} \le exp^{\left(\frac{-\Delta V_{HSTH(C/E)}}{gI_{spH}}\right)} exp^{\left(\frac{-\Delta V_{HSTL}}{gI_{spL}}\right)} \tag{3}$$

which can be simplified to give

$$\frac{I_{spL}}{I_{spH}} \ge \frac{\Delta V_{HSTL}}{\Delta V_{H(C/E)} - \Delta V_{HSTH(C/E)}} \tag{4}$$

confirming that a critical specific impulse ratio can be determined for the condition when the high-thrust fuel consumption is equal to the HST fuel consumption. Thus, for a given set of initial conditions, any specific impulse ratio above this critical value will be more fuel-efficient than the compared transfer.

From Eq. (4) it can be seen that, for the condition when the HST high-thrust ΔV equals that of the high-thrust only ΔV, a singularity exists. Beyond this signifies the region where the HST requires more fuel than the high-thrust only transfer and would be required to add mass to the system rather than remove it.

ANALYTICAL LOW-THRUST INCLINATION CHANGE METHODOLOGY

In order to consider the inclination change performed by the low-thrust system analytically, it is necessary to define the rate of change of inclination using the Gauss form of the Lagrange Planetary Equations, in terms of a spacecraft centered RTN coordinate system [4]. This is defined as

$$\frac{di}{dv} = \frac{r_c^3}{\mu p} \cos(v + \omega) N \tag{5}$$

where, for a circular orbit using the HST

$$p = r_c \tag{6}$$

As this analysis is based on a circular intermediate orbit and the argument of perigee is of no importance, it is assumed to be 90° to avoid the problem of it being undefined. This equation can then be integrated over one orbit to give the change in inclination. However, as the locally optimal control law states that the normal thrust switches sign depending on the argument of latitude, the integration is performed in two parts, from $0 - \pi$ and $\pi - 2\pi$. Eq. (7) represents the overall inclination change over one orbit, a result of summing the magnitudes from each integration.

$$\Delta I_{po} = \frac{4r_c^2 N_F}{\mu} \tag{7}$$

This can then be used with the orbital period and number of orbits required, defined respectively as

$$t_{period} = 2\pi \sqrt{\frac{r_c^3}{\mu}} \tag{8}$$

and

$$NOO = \frac{\Delta I}{\Delta Ipo} \tag{9}$$

to give the ΔV for the inclination change as shown in Eq. (10).

$$\Delta V_{HSTIL} = N_F t_{period} NOO \tag{10}$$

This can then be summed with the ΔV required to perform the low-thrust orbit transfer given in Eq.(11), and by introducing the orbit ratios $R1 \left(= \frac{r_t}{r_i}\right)$ and $R2 \left(= \frac{r_c}{r_i}\right)$ can be simplified to give the total ΔV used by the low-thrust system as shown in Eq. (12). It should be noted that Eq. (11) is an approximation for the low-thrust ΔV.

$$\Delta V_{HSTSL} = \sqrt{\frac{\mu}{r_t}} - \sqrt{\frac{\mu}{r_c}} \tag{11}$$

$$\Delta V_{HSTL} = \sqrt{\frac{\mu}{r_t}} \left[1 - \sqrt{\frac{R1}{R2}} + \sqrt{\frac{R1}{R2}} \frac{\pi}{2} \Delta I \right] \tag{12}$$

This equation can be used in the comparison of different initial orbits and transfers as the low-thrust section is constant in all cases. A visual representation of the transfer can be found in Figure 1.

ANALYTICAL HIGH-THRUST INCLINATION CHANGE METHODOLOGY

As is commonly known, it is more efficient to impart a plane change and orbit raise as part of the same maneuver, compared to carrying out each sequentially, when using a high-thrust system[5]. The ΔV required to perform the transfer is therefore calculated by comparing the initial and final orbit velocity vectors as well as the inclination plane change required. This is done using the cosine law as part of vector analysis. Figure 1 highlights the transfer specification while Eq. (13) details the ΔV equation.

$$\Delta V_{(a/b)} = \sqrt{v_{initial/final}^2 + v_{trans_{(a/b)}}^2 - 2v_{initial/final}v_{trans_{(a/b)}} \cos(\Delta I)} \tag{13}$$

As the transfer is conducted using two impulses, one to enter the transfer orbit and one to capture the target orbit, it is necessary to determine how much inclination change to impart at each impulse of the maneuver. An analytical approximation of this has already been established to an accuracy of $0.5°$ which introduces a scaling term, s, to represent the inclination imparted at each impulse as shown in Eq. (14)[5].

$$\Delta V = \Delta V_a + \Delta V_b = \sqrt{v_{initial}^2 + v_{trans_a}^2 - 2v_{initial}v_{trans_a} \cos(s\Delta I)} +$$
$$\sqrt{v_{final}^2 + v_{trans_b}^2 - 2v_{final}v_{trans_b} \cos((1-s)\Delta I)} \tag{14}$$

Firstly, squaring the two velocities to remove the square roots and ignoring the cross product terms $(2\Delta V_a \Delta V_b)$ gives

$$\Delta V_a{}^2 + \Delta V_b{}^2 \approx v_{initial}{}^2 + v_{trans_a}{}^2 - 2v_{initial}v_{trans_a}\cos(s\Delta I) + v_{final}{}^2 + v_{trans_b}{}^2 - 2v_{final}v_{trans_b}\cos\big((1-s)\Delta I\big)$$

This can then be differentiated with respect to s and set equal to zero:

$$\frac{\partial\left(\Delta V_a{}^2 + \Delta V_b{}^2\right)}{\partial s} \approx \Delta I 2v_{initial}v_{trans_a}\sin(s\Delta I) - \Delta I 2v_{final}v_{trans_b}\sin\big((1-s)\Delta I\big) = 0$$

By collecting terms and rearranging:

$$\frac{\sin(s\Delta I)}{\cos(s\Delta I)} \approx \frac{v_{final}v_{trans_b}\sin(\Delta I)}{v_{initial}v_{trans_a} + v_{final}v_{trans_b}\cos(\Delta I)}$$

Which then, with further simplification gives

$$s \approx \frac{1}{\Delta I}\tan^{-1}\left[\frac{\sin(\Delta I)}{X + \cos(\Delta I)}\right] \tag{15}$$

Where $X = \dfrac{v_{initial}v_{trans_a}}{v_{final}v_{trans_b}}$

Note that X can be modified, depending on the transfer scenario under consideration, by introducing the velocity formulas and simplifying with respect to the orbit ratios. For each transfer considered in this section this is accounted for and X is adjusted accordingly.

HOHMANN AND HST CRITICAL SPECIFIC IMPULSE RATIO WITH LOW-THRUST INCLINATION CHANGE (CIRCULAR INITIAL ORBIT)

The high-thrust only ΔV used to represent the Hohmann transfer in the comparison is given in Eq. (16). The high and low-thrust sections of the HST, both with a circular initial orbit, are defined in Eq. (17) and (12) respectively.

$$\Delta V_{HC} = \sqrt{\frac{\mu}{r_i} + \frac{2\mu r_t}{r_i(r_i+r_t)} - 2\sqrt{\frac{\mu}{r_i}}\sqrt{\frac{2\mu r_t}{r_i(r_i+r_t)}}\cos\left(tan^{-1}\left[\frac{sin(\Delta I)}{\sqrt{R1^3}+cos(\Delta I)}\right]\right)} +$$
$$\sqrt{\frac{\mu}{r_t} + \frac{2\mu r_i}{r_t(r_i+r_t)} - 2\sqrt{\frac{\mu}{r_t}}\sqrt{\frac{2\mu r_i}{r_t(r_i+r_t)}}\cos\left(\Delta I - tan^{-1}\left[\frac{sin(\Delta I)}{\sqrt{R1^3}+cos(\Delta I)}\right]\right)} \tag{16}$$

$$\Delta V_{HSTHC} = \sqrt{\frac{2\mu}{r_i} - \frac{2\mu}{r_i+r_c}} - \sqrt{\frac{\mu}{r_i}} + \sqrt{\frac{\mu}{r_c}} - \sqrt{\frac{2\mu}{r_c} - \frac{2\mu}{r_i+r_c}} \tag{17}$$

By substituting the orbit ratios defined previously, Eq. (4) reduces to give the critical ratio for the scenario, when the low-thrust system performs the inclination change, as defined in Eq. (18).

$$\frac{I_{spL}}{I_{spH}} = I_{sp}{}^{HHL-} = \frac{1-\sqrt{\frac{R1}{R2}}+\frac{\pi}{2}\sqrt{\frac{R1}{R2}}\Delta I}{\sqrt{R1}\mathcal{A}_1+\mathcal{A}_2-\mathcal{A}_3+\mathcal{A}_4-\sqrt{\frac{R1}{R2}}+\sqrt{R1}} \tag{18}$$

Where

$$\mathcal{A}_1 = \sqrt{1+\frac{2R1}{1+R1}-\sqrt{\frac{8R1}{1+R1}}cos\left(tan^{-1}\left(\frac{sin(\Delta I)}{\sqrt{R1^3}+cos(\Delta I)}\right)\right)}$$

$$\mathcal{A}_2 = \sqrt{1+\frac{2}{1+R1}-\sqrt{\frac{8}{1+R1}}cos\left(\Delta I-tan^{-1}\left(\frac{sin(\Delta I)}{\sqrt{R1^3}+cos(\Delta I)}\right)\right)}$$

$$\mathcal{A}_3 = \sqrt{2R1-\frac{2R1}{1+R2}}$$

$$\mathcal{A}_4 = \sqrt{\frac{2R1}{R2}-\frac{2R1}{1+R2}}$$

Equation (18) now gives a critical ratio that is dependent on only three variables; $R1$, $R2$ and ΔI. If the target orbit and inclination are known then the equation is only dependent on $R2$ or more specifically, the intermediate circular orbit radius value, r_c. Varying this will give a range of critical ratios where the HST using the low-thrust system to perform the inclination change, is equivalent in terms of fuel mass fraction to that of the Hohmann transfer utilizing a high-thrust inclination change. It should be noted that for this analytical approach it is assumed that the low-thrust system first performs the inclination change at the intermediate circular orbit before then spiraling in towards the target. This is a reasonable assumption based on the fact that the low-thrust ΔV for a plane change is at a minimum at the furthest point from the central body. This method will be validated later in this paper to ensure the assumption is credible. Figure 2 highlights $I_{sp}{}^{HHL-}$ for a varying $R2$ and ΔI and it can be seen that the critical ratio drops off with an increasing inclination change suggesting that the HST is more effective at larger inclination changes. Figure 3 displays the same critical equation but for a fixed $R1$ and $R2$ with changing inclination. It can be seen that $I_{sp}{}^{HHL-}$ tends to a constant value, with an inclination change greater than approximately 1.6 radians (90°).

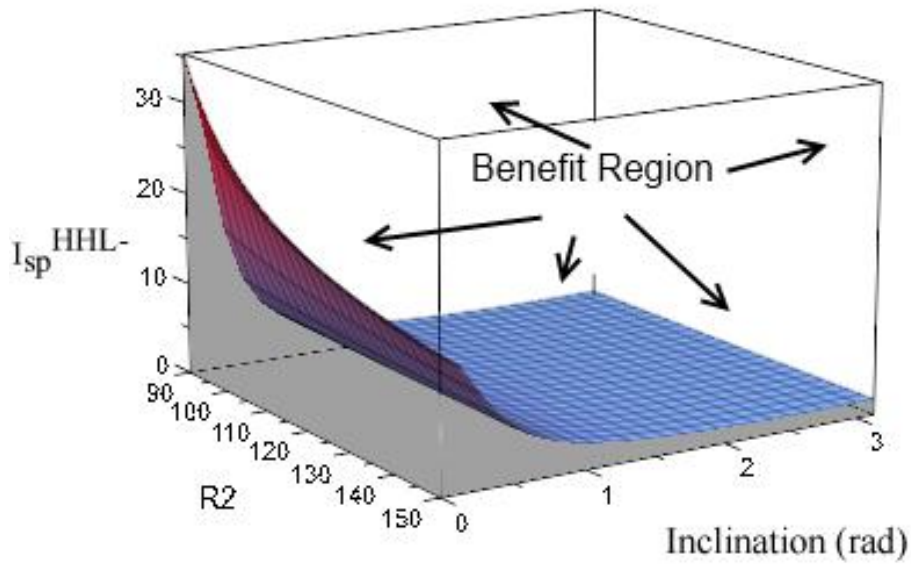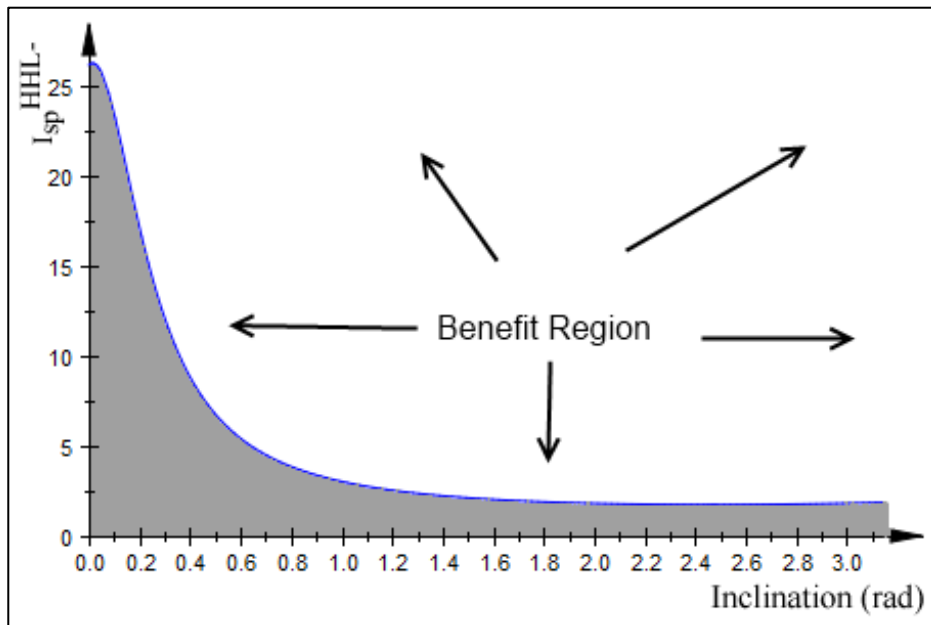**Figure 2. I_{sp}^{HHL-} Characteristics (R1=6.36)**

Figure 3. I_{sp}^{HHL-} Characteristics (R1=6.36, R2=100)

HOHMANN AND HST CRITICAL SPECIFIC IMPULSE RATIO WITH LOW-THRUST INCLINATION CHANGE (ELLIPTICAL INITIAL ORBIT)

For the case when the spacecraft starts in an elliptical orbit and the low-thrust section of the HST performs the inclination change, the high-thrust only Hohmann ΔV is given in Eq. (19) and accounts for a single impulse burn at apogee. This burn circularizes the orbit while also changing the inclination. It should be noted that the analytical analysis is only valid when the apogee of the initial orbit coincides with the final orbit radius. This is a reasonable assumption as it is

representative of a standard Geostationary Transfer Orbit (GTO) to Geostationary Earth Orbit (GEO). The low-thrust section of the HST is equal to Eq. (12). The high-thrust section of the HST is given in Eq. (20).

$$\Delta V_{HE} = \sqrt{\frac{2\mu r_i}{r_t(r_i+r_t)} + \frac{\mu}{r_t} - 2\sqrt{\frac{2\mu r_i}{r_t(r_i+r_t)}}\sqrt{\frac{\mu}{r_t}}\cos(\Delta I)} \tag{19}$$

$$\Delta V_{HSTHE} = \sqrt{\frac{2\mu r_c}{r_i(r_i+r_c)}} + \sqrt{\frac{\mu}{r_c}} - \sqrt{\frac{2\mu r_t}{r_i(r_i+r_t)}} - \sqrt{\frac{2\mu r_i}{r_c(r_i+r_c)}} \tag{20}$$

By then using the orbit ratios as previously defined and Eq. (4), the critical specific impulse ratio is given in Eq. (21).

$$\frac{I_{spL}}{I_{spH}} = I_{sp}{}^{HHLE} = \frac{1-\sqrt{\frac{R1}{R2}}+\frac{\pi}{2}\sqrt{\frac{R1}{R2}}\Delta I}{\mathcal{B}_1 - \sqrt{\frac{R1}{R2}}\mathcal{B}_2} \tag{21}$$

where,

$$\mathcal{B}_1 = \sqrt{\frac{2}{1+R1} + 1 - 2\sqrt{\frac{2}{1+R1}}\cos(\Delta I)}$$

$$\mathcal{B}_2 = \sqrt{R2}\left(\sqrt{\frac{2R2}{1+R2}} - \sqrt{\frac{2R1}{1+R1}}\right) - \sqrt{\frac{2}{1+R2}} + 1$$

The critical specific impulse ratio is now only dependent on $R1$, $R2$ and ΔI. If the target orbit and inclination are known then this equation is only dependent on $R2$ or more specifically, the intermediate circular orbit radius value, r_c. Varying this will give a range of critical specific impulse ratios that determine when the HST is equivalent, in terms of fuel mass fraction, to the Hohmann transfer. The comparison of the HST with the Hohmann transfer using the low-thrust system to implement the inclination change and starting in an elliptical orbit is very similar to the same case starting in a circular initial orbit. Figure 4 highlight the characteristics of $I_{sp}{}^{HHLE}$ showing that with increasing inclination change the HST's efficiency improves highlighted by the critical ratio becoming smaller. It can be seen that the elliptical and circular initial orbit critical equations display very similar characteristics.
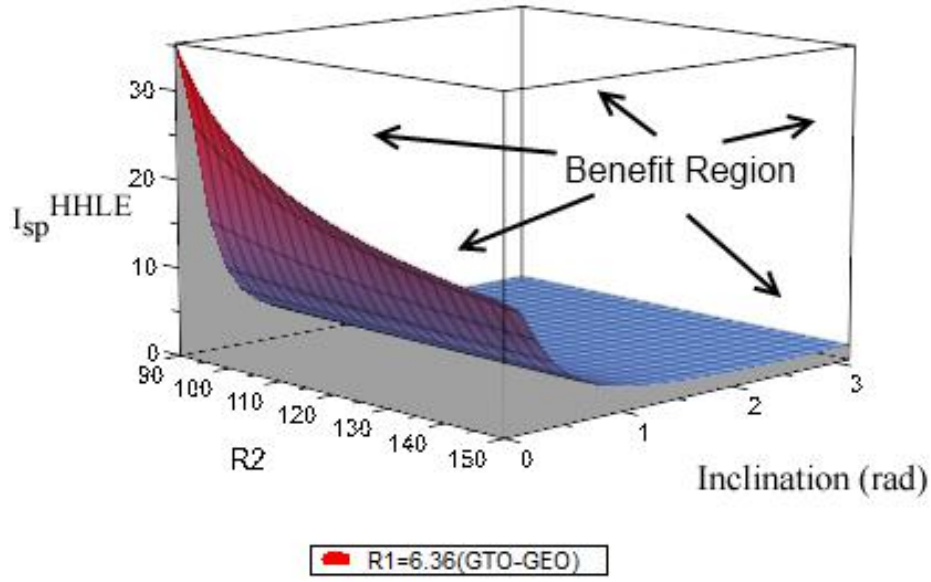
Figure 4 I_{sp}^{HHLE} characteristics (R1=6.36)

HST CRITICAL SPECIFIC IMPULSE RATIO

In order for a full comparison of the HST utilizing both high and low-thrust propulsion to implement an inclination change an additional critical ratio, dependent on the specific impulse again, can be derived which used in collaboration with the HST and Hohmann critical ratio, will give a full overview of the system. The critical ratio can be derived by comparing the fuel mass fraction, given Eq. (2), for each HST transfer configuration. The critical ratio, with little simplification, is then defined in Eq. (22) and is relevant for both a circular and elliptical initial orbit as only the ΔV equations will vary. The ΔV equations representing the HST utilizing high-thrust inclination change can be found in Reference 1.

$$\left.\frac{I_{spL}}{I_{spH}}\right|_{HST} = \frac{\Delta V_{HSTHL} - \Delta V_{HSTL}}{\Delta V_{HSTH(C/E)} - \Delta V_{HSTHH(C/E)}} \tag{22}$$

By substituting the relevant equations in, the critical specific impulse ratio comparing the HST utilizing high-thrust inclination change with its counterpart for a circular initial orbit is then defined in Eq. (23).

$$\left.\frac{I_{spL}}{I_{spH}}\right|_{HST} = I_{sp}^{HSH-} = \frac{-\frac{\pi}{2}\sqrt{\frac{R1}{R2}}\Delta I}{\sqrt{2R1 - \frac{2R1}{1+R2}} - \sqrt{\frac{2R1}{R2} - \frac{2R1}{1+R2}} - C_1 + C_2} \tag{23}$$

where

$$C_1 = \sqrt{R1}\left[1 + \sqrt{1 + \frac{2R2}{1+R2} - \sqrt{\frac{8R2}{1+R2}}\cos\left(tan^{-1}\left[\frac{sin(\Delta I)}{\sqrt{(R2)^3}+cos(\Delta I)}\right]\right)}\right]$$

$$C_1 = \sqrt{\frac{R1}{R2}}\left[1 - \sqrt{1 + \frac{2}{1+R2} - \sqrt{\frac{8}{1+R2}}\cos\left(\Delta I - tan^{-1}\left[\frac{sin(\Delta I)}{\sqrt{(R2)^3}+cos(\Delta I)}\right]\right)}\right]$$

Similarly, the critical specific impulse ratio, comparing the HST utilizing high-thrust inclination change and its counterpart for an elliptical initial orbit is defined in Eq. (24) with only the relevant ΔV's changing.

$$\left.\frac{I_{spL}}{I_{spH}}\right|_{HST} = I_{sp}^{HSHE} = \frac{-\frac{\pi}{2}\sqrt{\frac{R1}{R2}}\Delta I}{\sqrt{\frac{R1}{R2}}[\mathcal{D}_1 - \mathcal{D}_2 - \mathcal{D}_3]} \tag{24}$$

where

$$\mathcal{D}_1 = \sqrt{R2}\left(\sqrt{\frac{2R2}{1+R2}} - \sqrt{\frac{2R1}{1+R1}}\right) - \sqrt{\frac{2}{1+R2}} + 1$$

$$\mathcal{D}_2 = \sqrt{R2}\left[1 - \sqrt{\frac{2R1}{1+R1} + \frac{2R2}{1+R2} - \sqrt{\frac{8R1}{1+R1}}\sqrt{\frac{2R2}{1+R2}}\cos\left(tan^{-1}\left[\frac{sin(\Delta I)}{\sqrt{\frac{2R1R2^3}{1+R1}}+cos(\Delta I)}\right]\right)}\right]$$

$$\mathcal{D}_3 = \sqrt{1 + \frac{2}{1+R2} - \sqrt{\frac{8}{1+R2}}\cos\left(\Delta I - tan^{-1}\left[\frac{sin(\Delta I)}{\sqrt{\frac{2R1R2^3}{1+R1}}+cos(\Delta I)}\right]\right)}$$

NUMERICAL METHOD

Locally Optimal Control Laws

There are seven locally optimal control laws which can be used to optimize a trajectory; however as a general analysis of the HST without insertion requirements etc. requires only the semi-major axis, eccentricity and inclination, only these control laws will be introduced. As the rate of change of an element can be easily calculated, a locally optimal control law can be generated. These control laws aim to maximize the instantaneous rate of the element and provide the required thrust vector in a closed analytical form. The advantage of these control laws is the speed at which they can be implemented in trajectory models. The disadvantage is the sub-optimal nature of them and how this affects the resulting solution[6]. The variational equation of the element concerned is shown in Eq. (25).

$$\frac{d\sigma}{dt} = \boldsymbol{f}.\hat{\boldsymbol{\lambda}}_{\sigma} \tag{25}$$

where σ represents the respective element. The required force, $\boldsymbol{f}$ in the Radial, Transverse and Normal Axes (RTN) to maximise the rate of change of σ is a unit vector defined by $\boldsymbol{\lambda}_{\sigma}$. By maximizing the force along $\boldsymbol{\lambda}_{\sigma,}$ the instantaneous rate of σ is also maximized.

Semi-Major Axis Control Law

The semi-major axis variational equation is given in Eq. (26) in classical elements

$$\frac{da}{dt} = \frac{2a^2}{\sqrt{\mu p}}[R \quad T \quad N]\begin{bmatrix} esin(v) \\ 1 + esin(v) \\ 0 \end{bmatrix} \tag{26}$$

By then identifying λ_a and converting to modified equinoctial elements[7], the maximized unit thrust direction vector is given in Eq. (27).

$$\lambda_a = \begin{bmatrix} esin(v) \\ 1 + esin(v) \\ 0 \end{bmatrix} = \begin{bmatrix} fsin(L) - gcos(L) \\ 1 + (fcos(L) + gsin(L)) \\ 0 \end{bmatrix} \tag{27}$$

This can now be used to generate a locally optimal control law which focuses on maximizing the semi-major axis. This is also known as the energy gain control law as it gives a locally optimal variation in orbit energy.

Eccentricity Control Law

The eccentricity variational equation is given in Eq. (28) and is defined in classical elements.

$$\frac{de}{dt} = \frac{p}{\mu}[R \quad T \quad N]\begin{bmatrix} sin(v) \\ cos(v) + cos(E) \\ 0 \end{bmatrix} \tag{28}$$

By identifying λ_e and converting to modified equinoctial elements, the maximized thrust direction vector is given in Eq. (29).

$$\lambda_e = \begin{bmatrix} sin(v) \\ cos(v) + cos(E) \\ 0 \end{bmatrix} = \begin{bmatrix} \frac{fsin(L) - gcos(L)}{\sqrt{f^2 + g^2}} \\ \frac{[fsin(L) + gcos(L)]\left[1 + \frac{r}{p}\right]}{\sqrt{f^2 + g^2}} + \frac{r\sqrt{f^2 + g^2}}{p} \\ 0 \end{bmatrix} \tag{29}$$

Inclination Control Law

The inclination control law varies to the previously defined. It depends only on the out of plane perturbation and as such a switching term is required in order to maintain the chosen rate of change, either positive or negative. It will change according to the argument of latitude. Eq. (30) gives the variational equation for inclination defined in classical elements.

$$\frac{di}{dt} = \frac{r}{\sqrt{\mu p}}[R \quad T \quad N]\begin{bmatrix} 0 \\ 0 \\ cos(v + \omega) \end{bmatrix} \tag{30}$$

Identifying λ_i, converting to modified equinoctial elements and applying the switching term as discussed, the maximized unit thrust direction vector is given in Eq. (31).

$$\lambda_i = \begin{bmatrix} 0 \\ 0 \\ sgn[\cos(v + \omega)] \end{bmatrix} = \begin{bmatrix} 0 \\ 0 \\ sgn\left[\frac{h\cos(L)+k\sin(L)}{\tau}\right] \end{bmatrix} \tag{31}$$

Control Law Blending Method

The blending method used to determine the final direction vector, based on the mission objectives, derives from a form of averaging that has previously been applied to solar sail trajectory design known as A^nD blending[6]. The method is adopted here to suit low-thrust technologies without the limitations of a sail i.e. the thrust can be directed in any direction as and when it is needed. The method calculates the deficit (time to target) of each control law based on the maximized thrust vector if it were solely used and assuming a constant rate of change. These are normalized with respect to the largest, resulting with each control law receiving a score between zero and one; zero meaning the control law has achieved its target and one meaning it is furthest, in terms of time, from its target value. The control laws are then multiplied by an optimized weighting constant, based on mission specification, before finally being blended using the averaging technique as is shown in Eq. (32). This now forms the maximized thrust direction unit vector; all symbols have the same meanings as previously discussed.

$$\lambda_b = \frac{\sum W_\sigma \hat{\lambda}_\sigma}{\sum W_\sigma} \tag{32}$$

where $\sigma = a, e, i$

As opposed to several other blending methods in which the optimization process calculates the weighting parameters as a function of time from the initial epoch[5,6], this method ensures that the optimized weighting constants are independent of time. It should be noted that not all control laws are multiplied by an optimized weighting constant if they are not required to achieve the mission specification. In the cases which they are required, the optimizer selects the constants in such a manner that the overall time of flight and fuel mass are minimized while still achieving the mission specification.

Optimization Method

The optimization method selected to determine the constants uses a constrained nonlinear optimization method adapting a sequential quadratic programming (SQP) method. This was selected as it has a strict feasibility with respect to the bounds meaning every iterative step is taken within the specified bounds[10]. This is necessary for this study as the constants cannot be negative otherwise the trajectory generation will fail. As a result the lower boundary remains always at zero.

Analytical Validation

It is necessary to validate the analytical approach to ensure it can be used for further analysis. To do this a benchmark comparison against the numerical model is necessary. Table 1 details the transfer specification used while Table 2 provides the results. It should be noted that the optimization process was not used to perform the benchmark, instead it was performed in two phases; the first phase used only the inclination control law to perform the plane change and the spiral-in second phase used the semi-major axis control law only.

Table 1. Validation Study Specification

Analysis Parameter	Value
Initial Orbit, r_i (km)	6,628
Target Orbit, r_t (km)	19,884
Intermediate Orbit, r_c (km)	33,140
R1	3
R2	5
Initial Mass, m_{wet} (kg)	554
Low-thrust system specific impulse, I_{spL} (s)	4,500
Thrust, T (mN)	150
Inclination Change, ΔI (rad)	0.5236 (30°)

It can be seen that the majority of the error is associated with the mass analysis section of the transfer while the transfer time errors for both the inclination change and spiral sections are less than 0.1%. If the overall error is considered, as in that associated with the total fuel mass and transfer time then it can be seen that the total error for both cases reduces with the fuel mass error less than 3%.

Table 2 Validation Results

Analysis Parameter	Numerical	Analytical	Absolute Error (%) w.r.t. Numerical
Inclination Change Fuel Mass, (kg)	35.8	33.88	5.57
Spiral Fuel Mass, (kg)	11.84	12.52	5.74
Inclination Change Transfer Time, (days)	121.8	121.93	0.11
Spiral Transfer Time, (days)	40.26	40.44	0.45
Total Fuel Mass, (kg)	47.64	46.4	2.6
Total Transfer Time, (days)	162.06	162.4	0.21

COMPARISON OF CRITICAL SPECIFIC IMPULSE RATIOS (CIRCULAR ONLY)

The critical ratio derived in Reference 1 and given in Eq. (33) represents the Hohmann and HST comparison with the high-thrust section implementing the inclination change. This can be compared with the low-thrust inclination change as defined in Eq. (18) to help determine when each transfer is better.

$$\frac{I_{spL}}{I_{spH}} = I_{sp}^{HHH-} = \frac{1 - \sqrt{\frac{R1}{R2}}}{\sqrt{R1}\left[\varepsilon_1 - \varepsilon_2 - \sqrt{\frac{1}{R2}}\varepsilon_3\right] + \varepsilon_4} \tag{33}$$

where

$$\varepsilon_1 = \sqrt{1 + \frac{2R1}{1+R1} - \sqrt{\frac{8R1}{1+R1}}\cos\left(\tan^{-1}\left[\frac{\sin(\Delta I)}{\sqrt{(R1)^3} + \cos(\Delta I)}\right]\right)}$$

$$\mathcal{E}_2 = \sqrt{1 + \frac{2R2}{1+R2} - \sqrt{\frac{8R2}{1+R2}} \cos\left(tan^{-1}\left[\frac{sin(\Delta I)}{\sqrt{(R2)^3}+cos(\Delta I)}\right]\right)}$$

$$\mathcal{E}_3 = \sqrt{1 + \frac{2}{1+R2} - \sqrt{\frac{8}{1+R2}} \cos\left(tan^{-1}\left[\Delta I - \frac{sin(\Delta I)}{\sqrt{(R2)^3}+cos(\Delta I)}\right]\right)}$$

$$\mathcal{E}_4 = \sqrt{1 + \frac{2}{1+R1} - \sqrt{\frac{8}{1+R1}} \cos\left(tan^{-1}\left[\Delta I - \frac{sin(\Delta I)}{\sqrt{(R1)^3}+cos(\Delta I)}\right]\right)}$$

As the comparison is of the same transfers, i.e. Hohmann and HST but with different methods of inclination change, then only the lower critical ratio has to be exceeded to ensure the HST outperforms the Hohmann as opposed to having to satisfy the higher of the critical ratios when comparing different transfer types[2,3]. By then using the additional critical equation defined in Eq. (23), comparing the HST with both high and low-thrust inclination change, it is clearly shown for an example of $R = 3.64$ and $\Delta I = 0.6\ rad\ (\cong 34.38°)$ in Figure 5 when the HST utilizing low-thrust inclination change will outperform its high-thrust counterpart. The light grey section represents the region in which the HST utilizing low-thrust inclination change will always be better, in terms of fuel mass fraction, than the Hohmann transfer and HST with high-thrust inclination change. The dark grey section represents the region in which the HST utilizing high-thrust inclination change will always be better, in terms of fuel mass fraction, than the Hohmann transfer and HST with low-thrust inclination change. In the white region the HST with high or low-thrust inclination change will never outperform the Hohmann transfer. In addition, it is seen there is an intersection between I_{sp}^{HHH-}, I_{sp}^{HHL-} and I_{sp}^{HSH-} at $R2 = 35.97$ which represents the point at which, for a critical specific impulse ratio of 18.54, both HST systems will be equivalent, in terms of fuel mass fraction, to the Hohmann transfer.
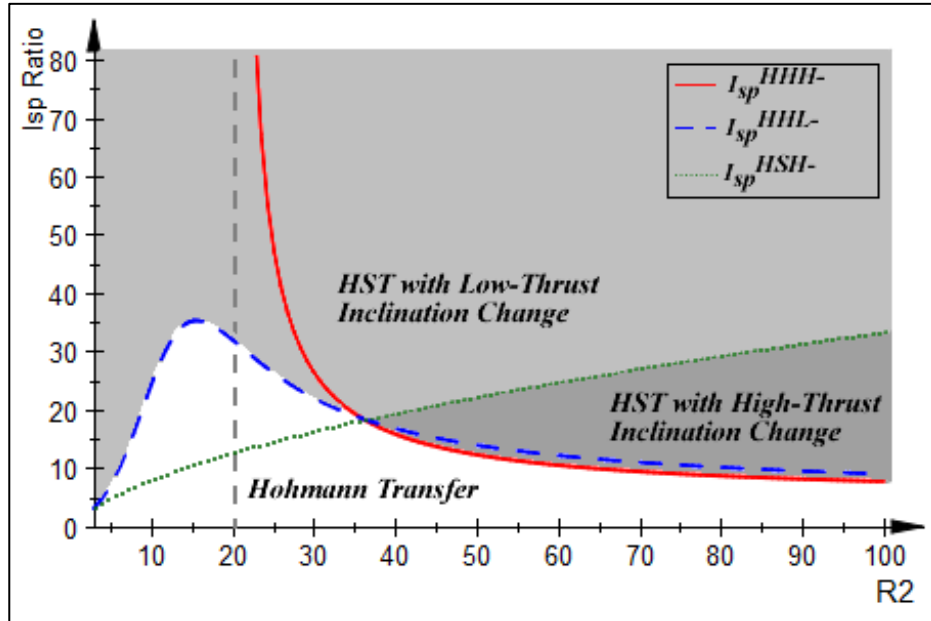

Figure 5 Critical Ratio Comparison, $R1 = 3.64$, $\Delta I = 0.6\ rad\ (\cong 34.38°)$

MASS ANALYSIS WITH TIME RESTRICTION

In order to perform a mission analysis it is necessary to determine the fuel mass required and total transfer time. This can be done numerically by substituting the ΔV for the low and high-thrust sections of the HST, as given in Eq. (12) and (17) respectively, into Eq. (2). Eq. (17) represents a circular initial orbit, if the elliptical initial orbit was to be studied Eq. (20) would have to be used. The fuel mass equation representing the circular initial orbit is given in Eq. (34).

$$\frac{m_{HSTF}}{m_{wet}} = 1 - exp\left(\frac{-\sqrt{\frac{\mu}{r_t}}\left[\sqrt{\frac{2R1R2}{1+R2}}+\sqrt{\frac{R1}{R2}}-\sqrt{\frac{2R1}{R2(1+R2)}}-\sqrt{R1}\right]}{gI_{spH}}\right) exp\left(\frac{-\sqrt{\frac{\mu}{r_t}}\left[1-\sqrt{\frac{R1}{R2}}+\sqrt{\frac{R1\pi}{R22}}\Delta I\right]}{gI_{spL}}\right) \tag{34}$$

The equation representing the total transfer time associated with the HST is given in Eq. (35). It should be noted that t_L accounts for both the inclination change and spiral transfer and assumes a constant acceleration based on the spacecraft mass after the high-thrust transfer section has been completed.

$$t_T = t_H + t_L \tag{35}$$

where

$$t_H = \frac{\pi}{\sqrt{\mu}}\sqrt{\left[\frac{r_t}{2R1}(1+R2)\right]^3}$$

$$t_L = \frac{\sqrt{\frac{\mu}{r_t}}\left[1-\sqrt{\frac{R1}{R2}}+\sqrt{\frac{R1\pi}{R22}}\Delta I\right]}{N_F}$$

These equations, coupled with the relevant critical specific impulse ratios can help give a full overview of a mission specification utilizing the HST and therefore help decide which transfer should be selected.

CONCLUSION

A critical specific impulse ratio defining the point at which the HST utilizing low-thrust inclination change is equivalent, in terms of fuel mass fraction, to a Hohmann transfer has been derived. Adopting a satellite configuration that exceeds this critical ratio will ensure that the HST offers a fuel mass benefit in comparison to the Hohmann only transfer. By using this critical ratio in conjunction with the ratio comparing the HST utilizing high-thrust inclination change and Hohmann transfer and the critical ratio comparing the two HST transfers, it can be determined which transfer offers the greatest fuel mass benefit depending on the satellite configuration and mission specification. Initial analyses have shown the HST utilizing low-thrust inclination change to offer the greatest benefit at low $R2$ ($R2 \rightarrow R1$) and large ΔI ($\Delta I > 30°$).

FUTURE WORK

To progress the analysis, the numerical optimization method will be used to optimize the HST transfer. This will allow the intermediate orbit to be varied and the inclination and spiral-in pahses to be combined. This should give benefits to both the fuel-mass and transfer time of the HST.

NOTATION

g – standard gravitational acceleration, m/s^2

μ - gravitational constant, m^3/s^2

m_{dry} – spacecraft mass without fuel, kg

m_{wet} – spacecraft mass with total fuel, kg

m_{HF} – high-thrust system fuel mass, kg

m_{HSTLF} – HST low-thrust section fuel mass, kg

m_{HSTF} – HST total fuel mass, kg

m_{02} – spacecraft mass after phase 1 of the HST transfer, kg

$\Delta V_{H(C/E)}$ – high-thrust only system with inclination change ΔV (circular/elliptical initial orbit), m/s

$\Delta V_{HSTH(C/E)}$ – high-thrust section of HST with low-thrust inclination change ΔV (circular/elliptical initial orbit), m/s

$\Delta V_{HSTHH(C/E)}$ – high-thrust section of HST with high-thrust inclination change ΔV (circular/elliptical initial orbit), m/s

ΔV_{HSTIL} – low-thrust inclination change section ΔV, m/s

ΔV_{HSTSL} – low-thrust spiral-in section ΔV, m/s

ΔV_{HSTL} – Total low-thrust section of HST ΔV with low-thrust inclination change, m/s

ΔV_{HSTHL} – low-thrust section of HST ΔV with high-thrust inclination change, m/s

$\Delta V_{(a/b)}$ – specified node ΔV between transfer and initial, m/s

ΔI – total inclination change, rad

ΔI_{po} – inclination change per orbit, rad

I_{spH} – high-thrust system specific impulse, s

I_{spL} – low-thrust system specific impulse, s

$v_{initial}$ – initial orbit velocity at beginning of specified transfer, m/s

v_{final} – target orbit velocity at end of specified transfer, m/s

$v_{trans(a/b)}$ – transfer orbit velocity at specified node, m/s

a_1 – semi-major axis between r_i and r_c

s – percentage inclination change at node a

r_i – initial orbit radius, m

r_t – target orbit radius, m

r_c – circular transfer orbit, m

a – semi-major axis, m

e – eccentricity

i – inclination, rad

p – semi-latus rectum, m

ω – argument of perigee, rad

υ – true anomaly, rad

E – eccentric anomaly

f – modified equinoctial element

g – modified equinoctial element

h – modified equinoctial element

L – modified equinoctial element

τ – auxiliary (positive) variable

σ – arbitrary orbit element

R – Radial Perturbation Component - RTN axis

T – Transverse Perturbation Component - RTN axis

N – Normal Perturbation Component - RTN axis

Tr – Thrust, mN

N_F – acceleration of low-thrust system based on m_{02}, m/s^2

NOO – number of orbits required for inclination maneuver

t – time, s

t_T – total HST transfer duration, seconds

t_H – HST transfer phase 1 duration (high-thrust), seconds

t_L – HST transfer phase 2 duration (low-thrust), seconds

t_{period} – orbital period, s

λ_σ – locally optimal orientation vector for element σ

λ_b – locally optimal orientation blended vector

W_σ – optimized weighting constant for each element σ

Table 3. Subscript Notation detailing transfer specification.

Transfer Comparison Type	Superscript (I_{sp}^{XXXX})
Hohmann compared with HST utilizing high-thrust system for inclination change	*HHH-*
Hohmann compared with HST utilizing low-thrust system for inclination change	*HHL-*
Hohmann compared with HST utilizing high-thrust system for inclination change *(elliptical initial orbit)*	*HHHE*
Hohmann compared with HST utilizing low-thrust system for inclination change *(elliptical initial orbit)*	*HHLE*
HST utilizing high-thrust system for inclination change compared with HST utilizing low-thrust system for inclination change	*HSH-*
HST utilizing high-thrust system for inclination change compared with HST utilizing low-thrust system for inclination change *(elliptical initial orbit)*	*HSHE*

ACKNOWLEDGEMENTS

REFERENCES

[1] Owens, S., and Macdonald, M., "An Extension and Numerical Analysis of the Hohmann Spiral Transfer," *International Astronomical Congress*, 2012.

[2] Owens, S., and Macdonald, M., "A Novel Method In Hybrid Propulsion Transfers," *International Astronomical Congress*, 2011, pp. 1–11.

[3] Owens, S., and Macdonald, M., "An Analogy to Bi-Elliptic Transfers Incorporating High and Low-Thrust," *Journal of Guidance, Control, and Dynamics (In Press)*, 2012.

[4] Fortescue, P., Stark, J., and Swinerd, G., *Spacecrat Systems Engineering*, 2003.

[5] Vallado, D. A., "Fundamentals of Astrodynamics and Applications," *Fundamentals of Astrodynamics and Applications*, Microcosm Press and Springer, 2007, pp. 319–389.

[6] Macdonald, M., "Analytical Methodologies for Solar Sail Trajectory Design," University of Glasgow, 2005.

[7] Walker Ireland, B and Owens, J, M. J. H., "A Set of Modified Equinoctial Orbit Elements," *Celestial Mechanics 36*, D. Reidel Publishing Company, 1985, pp. 409–419.

[8] Kluever, C., "Simple guidance scheme for low-thrust orbit transfers," *Journal of Guidance Control and Dynamics*, vol. 21, 1998, pp. 19–21.

[9] Schoenmakers, J., Pulido, J., and Jehn, R., *ESOC report S1-ESC-RP-5001*.

[10] Nocedal, J., and Wright, S. J., *Numerical Optimization*, Springer, 2003.